Inorg. Chem. **2007**, *46*, 6311–6318

A Theoretical Study of the Inner-Sphere Disproportionation Reaction Mechanism of the Pentavalent Actinyl Ions

Helen Steele*,† and Robin J. Taylor‡

Nexia Solutions, Hinton House, Warrington WA3 6AS, U.K., and Nexia Solutions, British Technology Centre, Sellafield, Seascale CA20 1PG, U.K.

Received February 7, 2007

The inner-sphere mechanisms of the disproportionation reactions of U(V), Np(V), and Pu(V) ions have been studied using a quantum mechanical approach. The U(V) disproportionation proceeds via the formation of a dimer (a cation–cation complex) followed by two successive protonations at the axial oxygens of the donor uranyl ion. Bond lengths and spin multiplicities indicate that electron transfer occurs after the first protonation. A solvent water molecule then breaks the complex into solvated $U(OH)_2^{2+}$ and UO_2^{2+} ions. Pu(V) behaves similarly, but Np(V) appears not to follow this path. The observations from quantum modeling are consistent with existing experimental data on actinyl(V) disproportionation reactions.

Introduction

The chemistry of the pentavalent actinyl ion (AnO_2^+) is highly important in understanding the behavior of actinides in the environment, wastes, and spent nuclear fuel processing. Under most environmental and process conditions, neptunium(V) is the dominant oxidation state of Np.[1] Plutonium(V), although substantially less stable, has been shown to be particularly important under environmental conditions and potentially in the aging of stored Pu stocks.[2] Except for a narrow pH range around 2−2.5,[3] uranium(V) is highly unstable, but it is important as a reaction intermediate in U redox reactions, such as photochemical and microbiological reductions of the highly stable U(VI) ion.[4] In the absence of other redox reagents, the stability of these actinyl(V) ions is governed by their disproportionation reactions, described in eq 1, in which the destabilizing effect of acidity is evident ($K \propto [H^+]^{-4}$). Interestingly, if we consider the primary solvation shell round the metal ions (but ignoring that around the proton), using generally accepted hydration numbers for actinide ions (An) in aqueous solution in the absence of complexing anions[5] the disproportionation reaction can be rewritten as eq 2, implying that during the reaction one or two additional solvent water molecules are required to satisfy the inner-sphere solvation shells of the products. While kinetic data exist on the rates of An(V) disproportionation reactions, a fundamental understanding of the mechanisms of these reactions remains obscure.[3] In particular, there are

* To whom correspondence should be addressed, E-mail: helen.steele@nexiasolutions.com.
† Nexia Solutions, Hinton House.
‡ Nexia Solutions, British Technology Centre.

(1) (a) Runde, W. *Los Alamos Sci.* **2000**, *26*, 392. (b) Drake, V. A. In *Science and Technology of Tributyl Phosphate*; Schulz, W. W., Burger, L. L., Navratil, J. D., Eds.; CRC Press: Boca Raton, 1990; Vol. 3, pp 123−147.

(2) (a) Nelson, D. M.; Lovett, M. B. *Nature* **1978**, *276*, 599. (b) Choppin, G. R.; Morgenstern, A. Plutonium in the Environment. In *Radioactivity in the Environment*; Kudo, A., Ed.; Elsevier: Amsterdam, 2001; Vol. 1, p 91. (c) Haschke, J. M.; Allen, T. H.; Morales, L. A. *Science* **2000**, *287*, 285. (d) Conradson, S. D.; Begg, B. D.; Clark, D. L.; Den Auwer, C.; Espinosa-Faller, F. J.; Gordon, P. L.; Hess, N. J.; Hess, R.; Keogh, D. W.; Morales, L. A.; Neu, M. P.; Runde, W.; Tait, C. D.; Viers, K.; Villella, P. M. *Inorg. Chem.* **2003**, *42*, 3715. (e) Conradson, S. D.; Abney, K. D.; Begg, B. D.; Brady, E. D.; Clark, D. L.; Den Auwer, C.; Ding, M.; Dorhout, P. K.; Espinosa-Faller, F. J.; Gordon, P. L.; Haire, R. G.; Hess, N. J.; Hess, R.; Keogh, D. W.; Lander, G. H.; Lupinetti, A. J.; Morales, L. A.; Neu, M. P.; Palmer, P. D.; Paviet-Hartmann, P.; Reilly, S. D.; Runde, W. H.; Tait, C. D.; Viers, D. K.; Wastin, F. *Inorg. Chem.* **2004**, *43*, 116.

(3) Weigl, F. In *The Chemistry of the Actinide Elements*; Katz, J. J., Seaborg, G. T., Morss, L. R., Eds.; Chapman and Hill: London, 1986; Vol. 1, p 169.

(4) Nagaishi, R.; Katsumura, Y.; Ishigure, K.; Aoyagi, H.; Yoshida, Z.; Kimura, T. *J. Photochem. Photobiol., A* **1996**, *96*, 45. (b) Renshaw, J. C.; Butchins, L. J. C.; Livens, F. R.; May, I.; Charnock, J. M.; Lloyd, J. R. *Environ. Sci. Technol.* **2005**, *39*, 5657.

(5) On the basis of EAS (Garnov, A. Yu.; Krot, N. N.; Bessonov, A. A.; Perminov, V. P. *Radiokhimiya* **1996**, *38*, 428.), EXAFS (Conradson, S. D.; Clark, D. L.; Neu, M. P.; Runde, W.; Tait, C. D. *Los Alamos Sci.* **2000**, *26*, 418.), quantum mechanical (Buhl, M.; Diss, R.; Wipff, G. *J. Am. Chem. Soc.* **2005**, *127*, 13506.), theoretical (Mauerhofer, E.; Zhernosekov, K.; Rösch, F. *Radiochim. Acta* **2004**, *92*, 5.), and crystal structure (Matonic, J. H.; Scott, B. L.; Neu, M. P. *Inorg. Chem.* **2001**, *40*, 2638.) data, it is likely that the actinyl ions exhibit a pentagonal bipyramidal structure in solution and that the trivalent and tetravalent actinide ions are surrounded by eight to nine water molecules in the inner sphere.

10.1021/ic070235c CCC: $37.00
Published on Web 07/11/2007

significant differences between U[6] and Pu[7] compared to Np[8] which are not understood at a fundamental level.

The very rapid disproportionation of U(V) has received considerable attention, initially being shown to be second order with respect to U(V) and approximately first order with respect to hydrogen ion concentration (eq 3, $n = 1$).[6a−c] Increasing ionic strength and complexing anions increases the rate of disproportionation,[6g,k] while U(VI) ions decrease the rate of disproportionation by the formation of a less reactive complex between U(V) and U(VI).[6i] Later work[6i,j] accounted for the effect of U(VI) by extrapolation of rate data to zero U(VI) concentration showing an appreciable deviation from the first-order relationship with $[H^+]$.

$$2AnO_2^{+} + 4H^{+} \leftrightarrow AnO_2^{2+} + An^{4+} + 2H_2O \qquad (1)$$

$$2AnO_2(H_2O)_5^{+} + 4H^{+} + (1-2)H_2O \leftrightarrow AnO_2(H_2O)_5^{2+} + An(H_2O)_{(8-9)}^{4+} \qquad (2)$$

Kern and Orleman proposed a mechanism of disproportion-

$$\frac{-d[An(V)]}{dt} = k[An(V)]^2[H^+]^n \qquad (3)$$

ation that involved an initial protonation step (eq 4) to form a UO_2H^+ ion, which then reacts with a further U(V) ion in the rate-limiting step (eq 5).[6b] This mechanism replicates the observed rate equation, where $k = K_{\chi_1}$. Duke and Pinkerton examined this mechanism, showing only a rather small enhancement of the rate in deuterated solutions, which indicated to them that the proton transfer required by this mechanism was highly improbable.[6e]

$$UO_2^{+} + H^{+} \overset{K}{\leftrightarrow} UO_2H^{2+} \qquad (4)$$

$$UO_2^{+} + UO_2H^{2+} \xrightarrow{\chi_1} UO_2^{2+} + UO_2H^{+} \qquad (5)$$

An alternative mechanism via the formation of a binuclear intermediate ($U_2^{V}O_4^{2+}$) followed by protonation was later shown to fit experimental rate data at variable acidity at least as well as a medium effect using Harned corrections or the Kern−Orleman mechanism.[6i,j] Indeed, Ekstrom[6j] notes that deuterium substitution enhances the values of the U(V)−U(VI) complexation and U(V) disproportionation rate constants almost identically compared with H_2O (by factors of 1.27 and 1.29, respectively), implying the similar role of water molecules in the formation of the U(V)−U(VI) and transition complexes, thus favoring the U(V) dimerization mechanism. The formation of such binuclear complexes, known traditionally in the literature as "cation−cation" interactions, is a specific feature of the chemistry of pentavalent actinyl ions in solution and solid states.[9] While no definitive solution-state structures have yet been characterized, solid-state crystal structures[9h−j] coupled with quantum mechanical studies,[9k,l] electronic absorption spectrophotometry,[9h] vibrational spectroscopy,[9c,f] X-ray scattering,[9d] NMR,[9e] Mossbauer spectroscopy,[9g] and other data, all indicate that these complexes involve the axial oxygen of a donor actinyl(V) ion bonding to another metal center. Later work,[6m] however, again reinterpreted both U(V) absorption spectra and the disproportionation mechanism.[6i,j,l]

Pu(V) is of an intermediate stability compared with U(V) and Np(V) and is most stable between pH 1 and 5. Ignoring complexities due to subsequent inter-plutonium-ion reactions,[7c,d] the basic Pu(V)−Pu(V) disproportionation reaction kinetics are similar to those of U(V) and also follow eq 3($n = 1$) in $HClO_4$.[7a] The same mechanism via an initial protonation to PuO_2H^{2+} followed by a rate-limiting reaction between this ion and another PuO_2^{+} ion has also been suggested to apply.[7a] Artyukhin[7b] showed that Pu(V) disproportionation in HNO_3 was very similar to that in $HClO_4$. Again, like U(V), studies in D_2O showed a small enhancement of the reaction rate ($k_{D_2O}/k_{H_2O} = 1.17$) inconsistent with a mechanism involving a hydrogen transfer at the slow stage.[7a]

Np(V) is far more stable than either U(V) or Pu(V) in aqueous solution, with an equilibrium constant for eq 1 equal to 4×10^{-7} M in 1 M $HClO_4$.[8h] Disproportionation is slow, compared to the reverse Np(IV)−Np(VI) reproportionation, and follows a different path to U(V) and Pu(V), with eq 3 ($n = 2$) applying.[8a−e] This is probably indicative of a mechanism in which two NpO_2H^{2+} ions interact in the slow

(6) (a) Kolthoff, I. M.; Harris, W. E. *J. Am. Chem. Soc.* **1946**, *68*, 1175. (b) Kern, D. M. H.; Orleman, E. F. *J. Am. Chem. Soc.* **1949**, *71*, 2102. (c) Kraus, K. A.; Nelson, F.; Johnson, G. L. *J. Am. Chem. Soc.* **1949**, *71*, 2510. (d) Kraus, K. A.; Nelson, F. *J. Am. Chem. Soc.* **1949**, *71*, 2517. (e) Duke, F. R.; Pinkerton, R. C. *J. Am. Chem. Soc.* **1951**, *73*, 2361. (f) Orleman, E. F.; Kern, D. M. H. *J. Am. Chem. Soc.* **1953**, *75*, 3058. (g) Imai, H. *Bull. Chem. Soc. Jpn.* **1957**, *30* (8), 873. (h) Casadio, S.; Lorenzini, L. *Anal. Lett.* **1973**, *6* (9), 809. (i) Newton, T. W.; Baker, F. B. *Inorg. Chem.* **1965**, *4* (8), 1166. (j) Ekstrom, A. *Inorg. Chem.* **1974**, *13* (9), 2237. (k) Koltunov, V. S. *The Kinetics of the actinide reactions;* Atomizdat: Moscow, 1974; p 70. (l) Bell, J. T.; Friedman, H. A.; Billings, M. R. *J. Inorg. Nucl. Chem.* **1974**, *36*, 2563. (m) Kaneki, H.; Fukotomi, H. *Bull. Res. Lab. Nucl. React.* **1980**, *5*, 27.

(7) (a) Rabideau, S. W. *J. Am. Chem. Soc.* **1957**, *79*, 6350. (b) Artyukhin, P. I.; Medvedovskii, V. I.; Gel'man, A. D. *Russ. J. Inorg. Chem.* **1959**, *4* (6), 596. (c) Koltunov, V. S. *The Kinetics of the actinide reactions;* Atomizdat: Moscow, 1974; p 236. (d) Cleveland, J. M. In *Plutonium Handbook: A Guide to the Technology*; Wick, O. J., Ed.; American Nuclear Society: La Grange Park, IL,1980; Vol. 1 & *2*, p 403.

(8) (a) Hindman, J. C.; Sullivan, J. C.; Cohen, D. *J. Am. Chem. Soc.* **1954**, *76*, 3278. (b) Sullivan, J. C.; Cohen, D.; Hindman, J. C. *J. Am. Chem. Soc.* **1957**, *79*, 4029. (c) Hindman, J. C.; Sullivan, J. C.; Cohen, D. *J. Am. Chem. Soc.* **1959**, *81*, 2316. (d) Koltunov, V. S.; Rykov, A. G. *Radiokhimiya* **1976**, *18* (1), 34. (e) Koltunov, V. S.; Zhuravleva, G. I.; Marchenko, V. I.; Tikhononov, M. F. *J. Inorg. Nucl. Chem. Suppl.* **1976**, 189. (f) Koltunov, V. S. *The Kinetics of the actinide reactions*; Atomizdat: Moscow, 1974; p 116. (g) Anan'ev, A. V.; Shilov, V. P.; Astafurova, L. N.; Bukhtiyarova, T. N.; Krot, N. N. *Radiokhimiya* **1989**, *31* (4), 52. (h) Fahey, J. A. In *The Chemistry of the Actinide Elements*; Katz, J. J., Seaborg, G. T., Morss, L. R., Eds.; Chapman and Hill: London, 1986; Vol. 1, p 443.

(9) (a) Sullivan, J. C.; Hindman, J. C.; Zielen, A. J. *J. Am. Chem. Soc.* **1961**, *83*, 3373. (b) Madic, C.; Guillaume, B.; Morisseau, J. C.; Moulin, J. P. *J. Inorg. Nucl. Chem.* **1979**, *41*, 1027. (c) Guillaume, B.; Begun, G. M.; Hahn, R. L. *Inorg. Chem.* **1982**, *21*, 1159. (d) Guillaume, B.; Hahn, R. L.; Narten, A. H. *Inorg. Chem.* **1983**, *22*, 109. (e) Glebov, V. A.; Tikhonov, M. F. *Koord. Khim.* **1982**, *8*, 48. (f) Belyaeva, A. A.; Dushin, R. B.; Sidorenko, G. V.; Suglobov, D. N. *Radiokhimiya* **1985**, *27*, 534. (g) Karraker, D. G.; Stone, J. A. *Inorg. Chem.* **1977**, *16*, 2979. (h) Krot, N. N.; Grigoriev, M. S. *Russ. Chem. Rev.* **2004**, *73*, 89. (i) Cousson, A.; Dabos, S.; Abzali, H.; Nectoux, F.; Pages, M. *J. Less-Common Met.* **1984**, *99*, 233. (j) Albrecht-Schmitt, T. E.; Almond, P. M.; Sykora, R. E. *Inorg. Chem.* **2003**, *42*, 3788. (k) McKee, M. L.; Swart, M. *Inorg. Chem.* **2005**, *44*, 6975. (l) Steele, H.; Taylor, R. J. *Inorg. Chem.* Submitted for publication.

stage (eqs 6 and 7),[8c−e] in this case $k = K^2\chi_2$. In the presence of complexing anions in aqueous (e.g., sulfate and oxalate ions) and nonaqueous solutions, disproportionation is accelerated and the equilibrium shifted toward Np(IV).[8b,f,g] Deuterated solutions again enhance the rate of Np(V) disproportionation by factors of 2.5−2.7, which has been related to a tighter bonding of hydrogen in the activated complex than in the NpO_2H^{2+} complex.[8c]

$$NpO_2^{+} + H^{+} \overset{K}{\leftrightarrow} NpO_2H^{2+} \quad (6)$$

$$NpO_2H^{2+} + NpO_2H^{2+} \xrightarrow{\chi_2} NpO_2^{2+} + Np(OH)_2^{2+} \quad (7)$$

It is clear that the kinetics of Np(V) disproportionation are different from those of U(V) and Pu(V) and that the mechanisms have not been properly established for any of these reactions. Protonation of the actinyl(V) ion followed by its interaction with either another protonated ion or free actinyl ion in the rate-limiting step has been proposed as well as an alternative mechanism via a U(V) dimer.

Theoretical approaches to the study of molecular structures using molecular dynamic studies,[10] ab initio,[11] and density functional approaches[12] are now well established for actinide ions but, more recently, these have been extended to the thermodynamics of ligand exchange,[13] the accurate modeling of the reduction of uranyl ions by iron(II) ions,[14] and further the electron exchange between U(VI) and U(V).[15]

Here, we report the first application of quantum modeling techniques to actinyl(V) disproportionation reactions, which assuming an inner-sphere interaction have enabled us to now suggest a mechanism for the U(V) and Pu(V) disproportionation reactions. It can be shown that the proposed inner-sphere mechanism agrees with the features of the experimentally observed reaction kinetics and also deals with the differences between U(V), Pu(V), and Np(V) disproportionation reactions.

Computational Detail

Grigoriev and co-workers[16] have isolated and structurally characterized the most basic Np(V) cation−cation (CC) complex, $NpO_2ClO_4(H_2O)_4$. This consists of infinite rows of Np(V) molecules and outer-sphere perchlorate counterions. Each Np(V) center has two CC interactions: one where it acts as a donor via an axial "yl" oxygen atom, and a second interaction in which it acts as an acceptor of a CC bond from the axial "yl" oxygen of a neighboring neptunyl ion. The remainder of its equatorial coordination plane consists of water molecules. This crystal structure can be used as a basic template to study quantum mechanically the CC interaction. Dimers were extracted from the $NpO_2ClO_4(H_2O)_4$ Grigoriev crystal structure. One CC bond terminated with H^+ ions, essentially replacing a neptunyl ligand by a water ligand. These extracted dimers were optimized at the HF and DFT levels of theory, and the DFT optimized structure is shown in Figure 1. Substitution of U(V,VI), Pu(V,VI), and Np(VI) into the Np(V) sites showed that in the An(V)−An(VI) complex the CC bond was ∼2.3 Å, and this was increased to 2.5 Å for An(V)−An(V) complexes.[9l] These gas-phase calculations compare to an experimental value of 2.35 Å.[16] For the An(V)−An(VI) type CC complexes, irrespective of the An ion, the minimum energy structure and wavefunction always corresponded to the acceptor An species, being the An(VI) ion with the An(V) ion acting as the donor actinyl. Experimentally, CC complexes of the actinides are dominated by Np(V) CC complexes[9h] with very few Pu(V) and U(V) CC complexes.[17] Our earlier theoretical calculations of the U(V) and Pu(V) analogues provide no explanation to this dominance and is simply being attributed to the greater stability of Np(V) compared to both U(V) and Pu(V) and to the increased practical difficulties in handling the more radioactive Pu complexes. Solution-phase measurements of stability constants show that CC complexes increase in stability in the order Am < Pu < Np < U.[9b,h]

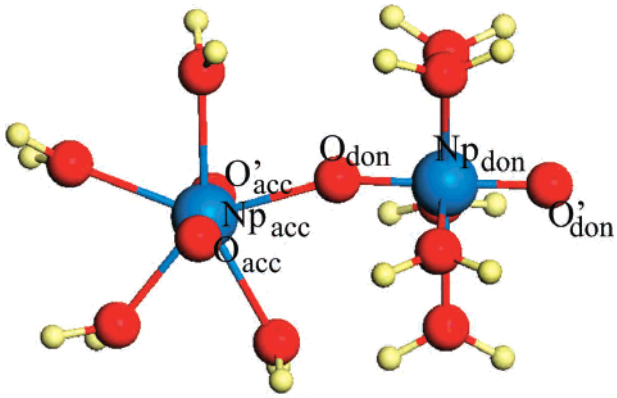

Figure 1. CC complex optimized at the B3LYP/SDD level.

In this study of An(V) ion disproportionation under acidic conditions, the essential chemical model described above (Figure 1) was the basis for all calculations. All starting coordinates were obtained from the crystal structure elucidated by Grigoriev including explicitly the first solvation shell. Secondary and higher solvation shells were not included as the disproportionation reactions were thought to be inner sphere.[6i,j] It is also accepted that the inclusion of

(10) (a) Durand, S.; Dognon, J.-P.; Guilbaud, P.; Rabbe, C.; Wipff, G. *J. Chem. Soc., Perkin Trans.* **2000**, *2*, 705. (b) Baaden, M.; Berny, F.; Madic, C.; Wipff, G. *J. Phys. Chem. A* **2000**, *104*, 7659.
(11) (a) Dolg, M.; Stoll, H. *Handbook on the Physics and Chemistry of Rare Earths*; Gschneider, K. A., Jr., Eyring, L., Eds.; Elsevier: Amsterdam, 1996; Vol. 22, p 152. (b) Tsuchiya, T.; Taketsugu, H.; Nakano, K.; Hirao, J. *J. Mol. Struct.* (*THEOCHEM*) **1999**, *461*, 203. (c) Vallet, V.; Schimmelpfennig, B.; Maron, L.; Teichteil, C.; Leininger, T.; Gropen, O.; Grenthe, I.; Wahlgren, U. *Chem. Phys.* **1999**, *244*, 185. (d) Ismail, N.; Heully, J.-L.; Saue, T.; Daudey, J.-P.; Marsden, C. *J. Chem. Phys. Lett.* **1999**, *300*, 296.
(12) (a) Hay, P. J.; Martin, R. L. *J. Chem. Phys.* **1998**, *109*, 3875. (b) Zhou, M.; Andrews, I.; Ismail, N.; Marsden, C. *J. Phys. Chem. A* **1998**, *104*, 5495. (c) Schreckenbach, G.; Hay, P. J.; Martin, R. L. *J. Comput. Chem.* **1999**, *20*, 70. (d) Maron, L.; Eisenstein, O. *J. Phys. Chem. A* **2000**, *104*, 7140.
(13) Vallet, V.; Wahlgren, U.; Schimmelpfennig, B.; Szabo, Z.; Grenthe, I. *J. Am. Chem. Soc.* **2001**, *123*, 11999.
(14) Tsushima, S.; Wahlgren, U.; Grenthe, I. *J. Phys. Chem. A* **2006**, *110*, 9175. (b) Wahlgren, U.; Tsushima, S.; Grenthe, I. *J. Phys. Chem. A* **2006**, *110*, 9025.
(15) Privalov, T.; Macak, P.; Schimmelpfennig, B.; Fromager, E.; Grenthe, I.; Wahlgren, U. *J. Am. Chem. Soc.* **2004**, *126*, 9801.
(16) Grigoriev, M. S.; Charushnikova, I. A.; Krot, N. N.; Yanovskii, A. I.; Struchkov, Y. T. *Zh. Neorg. Khim.* **1994**, *39*, 179.
(17) Burdet, F.; Pécaut, J.; Mazzanti, M. *J. Am. Chem. Soc.* **2006**, *128*, 16513.

solvation models is less essential for structural calculations than energetics and that the inclusion of such approaches within structural optimizations is both difficult and expensive.[13] All actinide complexes were optimized using Hartee−Fock (HF) and density-functional theory quantum mechanical (DFT) QM approaches using Gaussian03.[18] Due to the large number of electrons, pseudopotentials were used to represent the U, Np, and Pu centers. We utilized both the large core[19] (LC) (up to and including 4s and 5d electrons) and a [3s3p2d2f] contracted basis set for the remaining 14 electrons and the small core pseudopotentials of the Stuttgart type[20] (up to and including 4d and 4f) with a contracted Gaussian basis set of [10s,9p,5d,4f]. For all calculations, the electrons of the N, O, and H light elements were represented with a 6-31G(d) basis set and the requirement of polarization orbitals was assessed. Removal of the equatorial water ligands left a "T-complex"[9k] in which one O═An^{+}═O ion is linked to its partner actinyl ion by an axial oxygen bonding to the An metal center of the other ion in the equatorial plane. Optimization of this structure at the B3LYP/SDD level led to a CC separation of 2.45 Å. However, following spin annihilation the S^2 value was 2.66, which corresponds to a highly contaminated triplet wavefunction; no pure wavefunctions could be obtained. For optimization of the T-complex using an HF approximation, a noncontaminated wavefunction was obtained but the calculated CC separation was 2.12 Å. It was, therefore, concluded that to accurately study these complexes they were required to have complete equatorial planes, preventing the use of the most accurate but computationally intensive approaches. For all complexes, the high spin configuration was assumed throughout. Hence, for all the starting complexes, which are An(V)···An(V), the spin multiplicities ($2S + 1$) were 3 for U, 5 for Np, and 7 for Pu.

The $AnO_2^{+}\cdot 5H_2O$ molecules (Tables 1 and 2) and the CC complexes for U(V)···U(V), Np(V)···Np(V), and Pu(V)···Pu(V) interactions were optimized (Table 3). To simulate acid attack, H^{+} ions were placed at 0.97 Å from the bridging actinyl oxygens (step 1a, Figure 2). This bridging oxygen contains a higher δ-charge than the other actinyl axial oxygen atoms, but sterically it is more difficult to access. Therefore, attacks at both the bridging and end actinyl oxygens of the donor actinyl were modeled (step 1b, Figure 2). For the protonated donor species, the electronic structures were optimized using HF and DFT QM approaches with both SDD and LANL2DZ pseudopotentials. The optimum calculated

Table 1. Calculated Bond Distances for $[AnO_2(H_2O)_5]^{+}$ Complexes

chemical species	method	An═O (Å)	An−O_{water} (Å)
$[UO_2(H_2O)_5]^{+}$	HF/LANL2DZ	1.78	2.63
	/SDD	1.76	2.61
	B3LYP/LANL2DZ	1.81	2.61−2.62
	/SDD	1.81	2.57
	BPW91/SDD	1.82	2.58−2.59
$[NpO_2(H_2O)_5]^{+}$	HF/LANL2DZ	1.76	2.61
	/SDD	1.75	2.60−2.61
	B3LYP/LANL2DZ	1.81	2.60−2.65
	/SDD	1.79	2.53−2.57
	BPW91/SDD	1.81	2.56−2.62
$[PuO_2(H_2O)_5]^{+}$	HF/LANL2DZ	1.78	2.60
	/SDD	1.79	2.56−2.60
	B3LYP/LANL2DZ	1.81	2.58−2.66
	/SDD	1.79	2.56−2.60
	BPW91/SDD	1.79	2.55−2.63

Table 2. Calculated Bond Distances for $[AnO_2(H_2O)_5]^{2+}$ Complexes

chemical species	method	U═O (Å)	U−O_{water} (Å)
$[UO_2(H_2O)_5]^{2+}$	HF/LANL2DZ	1.69	2.54−2.55
	/SDD	1.69	2.52
	B3LYP/LANL2DZ	1.76	2.51
	/SDD	1.79	2.50
	BPW91/SDD	1.77	2.48
$[NpO_2(H_2O)_5]^{2+}$	HF/LANL2DZ	1.68	2.52−2.53
	/SDD	1.67	2.50
	B3LYP/LANL2DZ	1.76	2.50−2.52
	/SDD	1.73	2.46−2.47
	BPW91/SDD	1.76	2.46−2.47
$[PuO_2(H_2O)_5]^{2+}$	HF/LANL2DZ	1.66	2.51
	/SDD	1.66	2.50−2.51
	B3LYP/LANL2DZ	1.74	2.48−2.49
	/SDD	1.72	2.47
	BPW91/SDD	1.75	2.46

Table 3. CC and An═O Separations of the Optimized CC Complexes and Calculated Spin Densities

	CC (Å)	Ac_{acc}−O (Å)	Ac_{don}−O (Å)	Ac_{acc} spin	Ac_{don} spin
			HF/LANL2DZ		
U	2.51	1.81	1.86	1.20	1.21
		1.77	1.76		
Np	2.51	1.78	1.84	2.42	2.49
		1.78	1.76		
Pu	2.36	1.81	1.94	3.96	4.20
		1.85	2.04		
			DFT/LANL2DZ		
B3LYP					
U	2.52	1.85	1.89	1.22	1.23
		1.82	1.81		
Np	2.50	1.79	1.87	2.42	2.49
		1.83	1.80		
Pu	2.51	1.83	1.88	3.66	3.74
		1.80	1.80		
			DFT/SDD		
B3LYP					
U	2.44	1.80	1.90	1.11	1.11
		1.85	1.80		
Np	2.49	1.79	1.85	2.21	2.23
		1.80	1.78		
Pu	2.48	1.77	1.82	3.37	3.80
		1.80	1.76		
BPW91					
Np	2.48	1.81	1.86	2.19	2.25
		1.81	1.80		
Pu	2.48	1.78	1.86	3.34	3.40
		1.82	1.78		

(18) Frisch, M. J.; Trucks, G. W.; Schlegel, H. B.; Scuseria, G. E.; Robb, M. A.; Cheeseman, J. R.; Montgomery, J. A., Jr.; Vreven, T.; Kudin, K. N.; Burant, J. C.; Millam, J. M.; Iyengar, S. S.; Tomasi, J.; Barone, V.; Mennucci, B.; Cossi, M.; Scalmani, G.; Rega, N.; Petersson, G. A.; Nakatsuji, H.; Hada, M.; Ehara, M.; Toyota, K.; Fukuda, R.; Hasegawa, J.; Ishida, M.; Nakajima, T.; Honda, Y.; Kitao, O.; Nakai, H.; Klene, M.; Li, X.; Knox, J. E.; Hratchian, H. P.; Cross, J. B.; Bakken, V.; Adamo, C.; Jaramillo, J.; Gomperts, R.; Stratmann, R. E.; Yazyev, O.; Austin, A. J.; Cammi, R.; Pomelli, C.; Ochterski, J. W.; Ayala, P. Y.; Morokuma, K.; Voth, G. A.; Salvador, P.; Dannenberg, J. J.; Zakrzewski, V. G.; Dapprich, S.; Daniels, A. D.; Strain, M. C.; Farkas, O.; Malick, D. K.; Rabuck, A. D.; Raghavachari, K.; Foresman, J. B.; Ortiz, J. V.; Cui, Q.; Baboul, A. G.; Clifford, S.; Cioslowski, J.; Stefanov, B. B.; Liu, G.; Liashenko, A.; Piskorz, P.; Komaromi, I.; Martin, R. L.; Fox, D. J.; Keith, T.; Al-Laham, M. A.; Peng, C. Y.; Nanayakkara, A.; Challacombe, M.; Gill, P. M. W.; Johnson, B.; Chen, W.; Wong, M. W.; Gonzalez, C.; Pople, J. A. *Gaussian 03*, revision C.02; Gaussian, Inc.: Wallingford, CT, 2004.
(19) Hay, P. J.; Martin, R. L. *J. Am. Chem. Soc.* **1992**, *114*, 2736.
(20) Cao, X.; Dolg, M. *THEOCHEM* **2004**, *673*, 203−209.

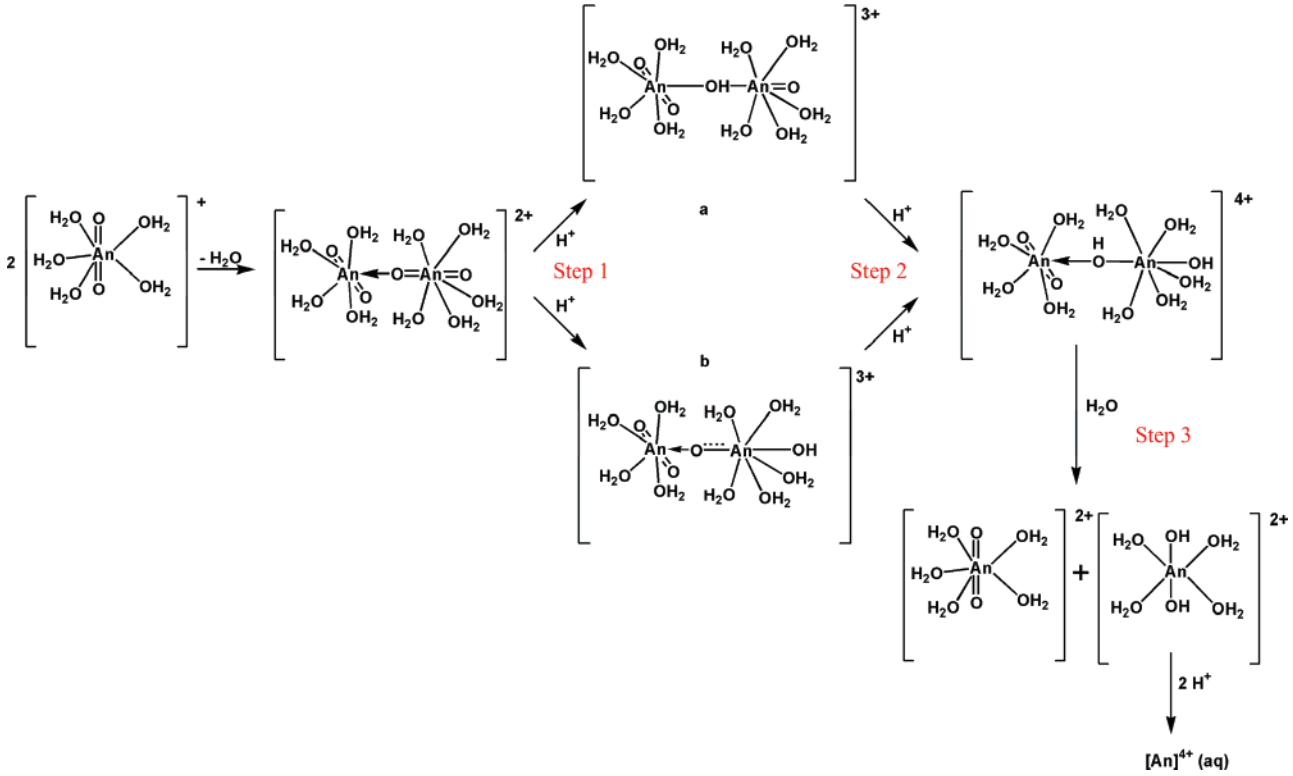

Figure 2. Schematic diagram of the An(V)−An(V) disproportionation reaction.

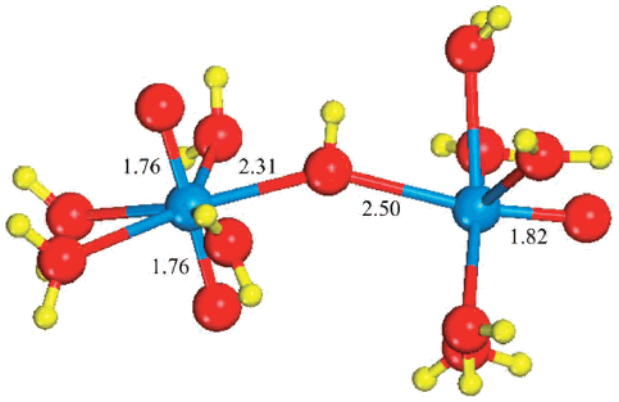

Figure 3. Protonated U···U complex optimized at the B3LYP/SDD level.

bond lengths and spin densities are given in Table 4. Following a second protonation (step 2, Figure 2) these doubly protonated complexes were reoptimized. As a result of doubly protonating the donor actinyl, an $\{An(OH)_2 \cdot 5H_2O\}$ grouping has been created with a potential energy barrier to the abstraction of the added H^+ ions; consequently, care was taken not to overinterpret the electronic structure following a second protonation. Calculations using a combination of HF (which does not include electron correlation) and a small core SDD pseudopotential frequently resulted in highly contaminated wavefunctions. Therefore, this combination was not used after the calculation of the unprotonated CC complexes.

To complete the disproportionation reaction in the U case, a water molecule was added to the equatorial plane of the acceptor U complex (step 3, Figure 2).

Results

$[AnO_2(H_2O)_5]^+$ Complexes. The calculated bond lengths for the optimized $AnO_2^{+/2+} \cdot 5H_2O$ ions are given in Tables 1 and 2. The initial coordinates prior to geometry optimization for the ions were taken from the $NpO_2ClO_4(H_2O)_4$ Grigoriev crystal structure,[16] and no symmetry constraints were implemented. At the B3LYP level employing an SDD pseudopotential and a 6-31G(d) basis set on the light elements, the calculated An═O separations were 1.81, 1.79, and 1.79 Å, respectively, which compare with UMP2 calculations[14] of 1.81, 1.77, and 1.74 Å and EXAFS values of 1.85 Å for Np[21] and 1.84 Å[22] for Pu; data for U(V) are unavailable. For the equivalent $AnO_2^{2+} \cdot 5H_2O$ complexes, the An═O separations were reduced to 1.79, 1.73, and 1.72 Å which compare to MP2/UMP2 calculated values of 1.76, 1.73, and 1.71 Å, and EXAFS measured values of 1.77 Å,[13] 1.76 Å[21] for U(VI), 1.75 Å[23] for Np(VI), and 1.74 Å[22] for Pu(VI). These calculated separations supported by the calculated spin densities have been used to assign the oxidation state of the actinide centers within the CC complexes.

Step 1: First Protonation of Uranium Dimer Complex. Protonation of the bridging "yl" oxygen of the uranyl(V) CC complex for both HF and B3LYP indicated a single electron transfer from the acceptor uranyl to the donor center, the electron transfer taking place prior to structural optimiza-

(21) Allen, P. G.; Bucher, J. J.; Shuh, D. K.; Edelstein, N. M.; Reich, T. *Inorg. Chem.* **1997**, *36*, 4676.
(22) Ankudinov, A. L.; Conradson, S. D.; De Leon, J. M.; Rehr, J. *J. Phys. Rev. B* **1998**, *57*, 7518.
(23) Reich, T.; Bernhard, G.; Geipel, G.; Funke, H.; Hennig, C.; Rossberg, A.; Matz, W.; Schell, N.; Nitsche, H. *Radiochim. Acta* **2000**, *88*, 633.

Table 4. CC and An=O Separations of the Optimized Protonated CC Complexes and Calculated Spin Densities

	CC (Å)	Ac_{acc}−O (Å)	Ac_{don}−O (Å)	Ac_{acc} spin	Ac_{don} spin
		HF/LANL2DZ			
U	2.41	1.70	2.63	0.00	2.10
		1.70	1.81		
Np	2.75	1.81	2.19	2.43	3.17
		1.75	2.13		
Pu	2.36	1.67	2.51	2.53	4.39
		1.67	1.81		
		DFT/LANL2DZ			
B3LYP					
U	2.35	1.77	2.46	0.01	2.34
		1.77	1.85		
Np	>5	1.80	2.01	2.41	2.66
		1.80	1.81		
Pu	2.70	1.85	2.14	3.60	4.09
		1.81	1.87		
		DFT/SDD			
B3LYP					
U	2.31	1.76	2.50	0.00	2.14
		1.76	1.82		
Np	>5	1.78	1.99	2.21	2.25
		1.79	1.76		
Np	>3	1.78	1.99	2.20	2.25
(END)		1.79	1.76		
Pu	>5	1.77	1.99	3.35	3.49
		1.77	1.77		
Pu	>3	1.75	1.78	3.34	3.51
(END)		1.80	1.96		
BPW91					
Np	>5	1.78	2.03	2.21	2.28
		1.78	1.79		
Np	2.58	1.79	1.88	1.79	2.69
(END)		1.78	2.01		
Pu	>5	1.78	1.98	2.37	4.32
		1.78	1.77		
Pu	2.50	1.76	1.88	2.65	3.42
(END)		1.79	1.99		

tion. The S^2 values were found to be 2.12 ± 0.09 (Table 3), as would be expected for a triplet structure, indicating that a complete electron transfer has taken place and the eigenfunctions are virtually pure spin states with no contamination from other spin states. The summation of the Mulliken population for the acceptor uranyl was +0.94 which compares well with +0.91 calculated for $UO_2{\cdot}5H_2O^{2+}$ complex. The calculated U=O bond lengths of the acceptor uranyl at the HF/SDD level were significantly lower from the initial lengths prior to protonation; from 1.81 and 1.77 Å to 1.70 Å which compares with 1.69 Å for the $[AnO_2(H_2O)_5]^{2+}$ molecule (Table 2). For B3LYP/SDD, the reduction went from 1.85 and 1.80 Å to 1.76 Å (Figure 3). Such separations in the acceptor uranyl correspond to the U(VI)−axial oxygen distance and, hence, the U(V)···U(V) CC complex has transformed to a U(VI)···U(IV) complex. This conclusion is further supported by no unpaired electrons being located on the acceptor U center (Table 3), both being assigned to the donor U. Prior to protonation, the $U_{acc}-O_{water}$ separation had a large range from 2.54 to 2.72 Å and the $U_{don}-O_{water}$ separation ranged from 2.48 to 2.55 Å.

Following protonation and electron transfer, the CC bond decreases from 2.51 to 2.41 Å, the axial acceptor O shortens to 1.70 Å for U(VI), and the An_{don}−O bond lengthens dramatically from a uranyl (V) length of 1.90 Å to an U−OH/water length of 2.63 Å. Both the range and the separation for the $U_{acc}-O_{water}$ center were reduced to between 2.50 and 2.57 Å, whereas the $U_{don}-O_{water}$ separation was increased to 2.57−2.58 Å. Upon acid attack, the CC separation for the B3LYP/SDD complex was reduced from 2.52 to 2.35 Å. The protonated structure was reoptimized with diffuse functions in the oxygen basis set (6-31G(d,f)) using an SDD pseudopotential and B3LYP functional, and the calculated value was in very good agreement with the 6-31G(d) basis set. The maximum change in bond lengths was a 0.03 Å increase. The calculated spin densities for U_{acc} and U_{don} centers were 0.03 and 2.10, respectively. Due to such small differences diffuse functions were not included further in this study. The vibrational frequencies (ν_1 and ν_3) were calculated using the B3LYP functional and an SDD pseudopotential. For the uranyl acceptor center, the calculated vibrational frequencies are 805 and 890 cm^{-1} prior to protonation and 915 and 1008 cm^{-1} following disproportionation. These compare with experimental values[24] for UO_2^{2+} of 869 and 965 cm^{-1}, MP2[25] calculated values of 923 and 1024 cm^{-1}, and B3LYP[26] calculated values for the unsolvated uranyl ion of 1041 and 1140 cm^{-1}. There were no negative vibrational frequencies calculated.

Step 2: Second Protonation of Uranium Dimer Complex. Protonation of the second "yl" oxygen of the U(IV)···U(VI) complex increased the CC separation; for B3LYP the increase was 0.45 Å. This second protonation did not alter the electron distribution between the two U centers.

Step 3: Addition of Water to Protonated Uranium Dimer. Introduction of a water molecule to the equatorial coordination shell of the doubly protonated uranyl complex finally broke the CC bond, and the two positively charged uranium centers repelled each other. This breaking of the CC bond occurred if the water molecule was introduced into the $U^{VI}O_2$ equatorial plane (at a separation of 2.65 Å). The simultaneous addition of two water molecules to both centers also broke the complex, but addition of a water molecule to only the coordination sphere of the $U^{IV}(OH)_2$ half of the complex actually decreased the CC bond from 2.55 to 2.48 Å and the CC complex remained intact. At the end of the geometry optimization the two stable U species were the pentagonal bipyramidal aquated uranyl(VI) ion, $UO_2{\cdot}5H_2O^{2+}$, and the twice hydrolyzed U(IV) ion, $U(OH)_2{\cdot}5H_2O$, which showed two U−OH separations of 2.34 Å and U−H_2O distances of 2.5 Å. The U(IV) center contained two unpaired electrons. It is assumed that the $U(OH)_2^{2+}$ ion further rapidly picks up one or two additional water molecules from the solvent to satisfy its inner coordination sphere (eight or nine coordinate).

Pu(V)···Pu(V) Complex. For the Pu(V)···Pu(V) complex at the HF level of theory, employing an LANL2DZ pseudopotential, protonation of the bridging oxygen led to electron transfer from Pu_{acc} to Pu_{don}, analogous to that observed for U. The Pu_{acc}=O separations were reduced from 1.81 and

(24) Allen, P. G.; Bucher, J. J.; Shuh, D. K.; Edelstein, N. M.; Reich, T. *Inorg. Chem.* **1997**, *36*, 4676.
(25) Majumdar, D.; Balasubramanian, K.; Nitsche, H. *Chem. Phys. Lett.* **2002**, *361*, 143.
(26) Zhou, M.; Andrews, L.; Ismail, N.; Marsden, C. *J. Phys. Chem. A* **2000**, *104*, 5495.

1.84 to 1.67 Å which compares to 1.66 Å for $PuO_2{\cdot}5H_2O^{2+}$ (Table 2). Pu_{don} carried an unpaired spin value of 4.39 (Table 4), which equates to Pu(IV). The calculated wavefunction contained a degree of spin contamination, and the former bridging oxygen carried a single unpaired electron. Protonation of the second oxygen caused the CC complex to break apart.

The B3LYP results did not agree with those obtained at the HF/LANL2DZ level. For B3LYP/LANL2DZ, there was partial electron transfer between the two Pu centers but the $Pu_{acc}{=}O_{acc}$ separations did not decrease. Following the second protonation at the end "yl" of the donor plutonyl (step 2, Figure 2), transfer of an electron from the Pu_{acc} center to Pu_{don} occurred. This protonation initiated the breaking of the CC interaction and, as they were no longer bound, the two positively charged species repelled each other. For B3LYP/SDD, the CC complex was broken following optimization of the singularly protonated complex, there was no transfer of electron density, and consequently the spin density was distributed evenly between the two Pu(V) centers, even if the first H^+ attack occurred at the less sterically hindered "yl" oxygen (step 1b, labeled (END) in Table 4). By use of a second DFT functional, including the non-hybrid-exchange functional of Becke[27] and the correlation functional of Perdew and Wang,[28] the CC complex and protonated structures were reoptimized.

For BPW91/SDD, acid attack at the bridging "yl" oxygen broke the CC bond but, unlike the B3LYP functional, Pu_{acc} had a spin density of 2.37 with Pu_{don} carrying a further two unpaired electrons (Table 4) leading to disproportionated Pu(VI) and Pu(IV) centers. There was only partial electron transfer when the end "yl" was attacked (step 1b), but the CC bond did not break enabling further H^+ to attack. Following this attack, the $Pu_{acc}{-}O_{acc}$ separation was significantly reduced to a value of 1.75 Å which is characteristic of Pu(VI). This second protonation also broke the CC interaction between the two Pu species. The $Pu_{acc}{-}O_{water}$ distances following disproportionation were all 2.42 Å. Unlike U disproportionation, no additional water molecules were required to complete the disproportionation reaction.

Np(V)···Np(V) Complex. Following a single protonation (step 1a) of the Np(V)···Np(V) CC complex, with optimization at the HF/LANL2DZ level, Np_{don} carried 0.74 more spin density than Np_{acc}; following a second protonation (step 2) this electron density returned to $Np_{acc.}$ After double protonation, both Np centers carried two unpaired electrons characteristic of Np(V). On use of the B3LYP functional, irrespective of the pseudopotential, there was no electron transfer associated with the protonation of the bridging "yl" oxygen of the Np(V)···Np(V) CC complex. Geometrical optimization of this complex at the B3LYP/SDD level broke the CC bond, with each Np center carrying just over two electrons (i.e., still Np(V)···Np(V)). Following geometrical optimization of the doubly protonated B3LYP/LANL2DZ complex, the CC bond was broken, with $Np_{acc}{=}O$ separations of 1.81 Å, and the wavefunction was severely contaminated.

(27) Becke, A. D. *J. Chem. Phys.* **1993**, *98*, 5648.
(28) Perdew, J. P.; Burke, K.; Wang, Y. *Phys. Rev. B* **1996**, *54*, 16533.

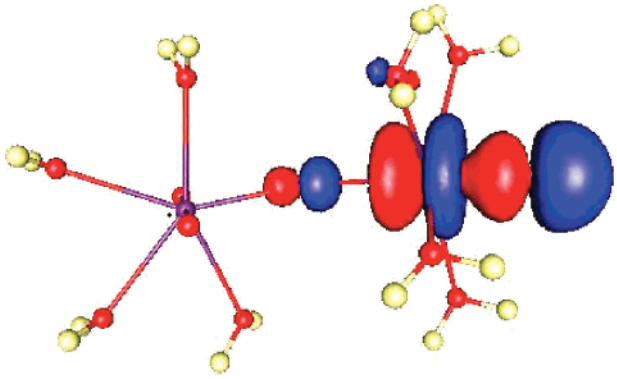

Figure 4. HOMO-2 for the B3LYP/SDD optimized singly protonated U CC complex.

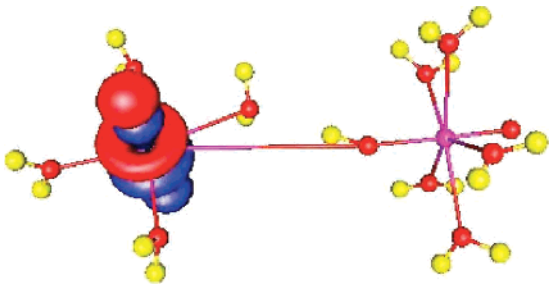

Figure 5. HOMO-2 for the B3LYP/SDD optimized singly protonated Np CC complex.

As with the Pu complexes, the Np CC complexes were also optimized using the BPW91 functional. H^+ attack at the bridging oxygen broke the CC complex. Following this breakup, the two Np centers both carried two unpaired electrons and the $Np_{acc}{-}O_{acc}$ distances were slightly shorter than in the unprotonated CC complex but were not reduced to those values found for the $[NpO_2(H_2O)_5]^{2+}$ ion (Table 2). Following attack at the end oxygen, Np_{acc} carried a spin density of 0.9 less than Np_{don} and this complex did not break up.

Calculations of the orbital occupancies of the CC complexes revealed that the highest occupied orbital located along the actinyl bond was the HOMO-2 for U, Np, and Pu CC complexes. In the case of the U CC complex (Figure 4) at the B3LYP/SDD level, this orbital lies along the axis of the donor actinyl ion pointing toward the second metal center. For the Np CC complexes, the HOMO-2 lies along the acceptor actinyl perpendicular to the CC bond. Hence, it is hypothesized that this orbital, lying along the CC bond for the U and Pu CC complexes, may facilitate the electron-transfer mechanism and explain the differing behavior of the An(V) CC complexes and their tendencies toward disproportionation.

Discussion

For the Pu calculations described in the Results above, there is a significant discrepancy in the calculated ground-state electron configuration between the B3LYP functional and the BPW91 functional. This has not been further examined in this paper, but it is noted that the main disparity is with the electron density on the Pu_{acc} center following a single protonation as shown in Table 4 with close agreement

in the Pu_{don} centers. The SDD small core pseudopotential leaves the 4s and 5d electrons in the valence regions and not parametrized into the core as with the LANL2DZ pseudopotential, and hence, results generated using the SDD can be expected to be more accurate. It has been previously noted that the large core pseudopotential is not always appropriate for doing DFT calculations[29,30] with the small core being preferable.

It has been reported that the presence of U(VI) ions inhibits the disproportionation[6i,j] reaction. Protonation of a U(V)···U(VI) complex at the HF/SDD and B3LYP/SDD levels broke the CC complex with no electron transfer between the two U centers, which would require a change in the multiplicity of the system. For the U(V)···U(V) complex, the spin multiplicity of the system is preserved throughout and, hence, the disproportionation reaction via this U(V)··•U(V) CC mechanism is spin allowed[31] and so favorable.

Overall, our inner-sphere mechanism for U(V) disproportionation is described by eqs 8−11, with electron transfer occurring after the first protonation (eq 9, step1, Figure 2). With the BPW91 functional, Pu(V) follows a similar path although the complex may break up after the electron transfer which appears to follow the second protonation (eq 10, step 2, Figure 2). Np(V) does not seem to follow this path, and the mechanism proposed by Hindman[8c] and Koltunov[8d,e] still seems probable. Assuming the first protonation step to be rate determining, this mechanism is consistent with the experimental U(V)[6] and Pu(V)[7] disproportionation kinetics.

$$AnO_2^{+} + AnO_2^{+} \leftrightarrow (AnO_2)_2^{2+} \quad (8)$$

$$(AnO_2)_2^{2+} + H^{+} \rightarrow (AnO_2)_2H^{3+} \quad (9)$$

$$(AnO_2)_2H^{3+} + H^{+} \rightarrow (HOAnOHOAnO)^{4+} \quad (10)$$

$$(HOAnOHOAnO)^{4+} \xrightarrow{H_2O} AnO_2^{2+} + An(OH)_2^{2+} \quad (11)$$

Conclusion

We have studied the inner-sphere disproportionation reaction for U(V), Np(V), and Pu(V) using the HF approach and two frequently used DFT functionals with both the LANL2DZ and SDD pseudopotentials. Presented in this paper are two very similar mechanisms for the disproportionation of U(V) and Pu(V) in the presence of protons and water. Incidentally, the roles of acid and water in the disproportionation reaction are exemplified by the study of uranyl disproportionation in nonaqueous phases, the half-life of U(V) being extended to about an hour in dry DMSO.[32]

A number of our key computational findings are supported by experimental observations. The suggested mechanism is dependent upon labile water molecules, and the loss of a water ligand from the equatorial plane of An_{acc} is essential to form the starting U(V)···U(V) CC complex,[33] and also, addition of a water molecule is required to break the CC interaction following disproportionation of the U complex. Slight variations were observed with Pu(V), as following electron transfer disproportionation formed coordinatinatively unsaturated $Pu(VI)O_2^{2+}•4H_2O$ molecules which require an extra water molecule to complete their equatorial plane. Second, the suggested mechanism for both U and Pu disproportionation reactions leads to formation of $An(OH)_2^{2+}$ ions as pseudostable products (these also require a further one or two water molecules from the solvent to complete their inner hydration sphere). These ions are frequently cited as probable intermediates in actinide redox reactions.[34] No definite mechanism has been suggested for the Np(V) disproportionation here, but in agreement with experimental data,[8] quantum mechanically it differs significantly from that of its neighboring actinides.

Acknowledgment. We thank The Nuclear Decommissioning Authority for funding and Dr. Mark Vincent and Professor David Collison (University of Manchester) for helpful discussions.

IC070235C

(29) Batista, E. R.; Martin, R. L.; Hay, P. J.; Perelta, J.; Scuseria, G. E. *J. Chem. Phys.* **2004**, *121*, 2144.
(30) Russo, T. V.; Martin, R. L.; Hay, P. J. *J. Phys. Chem.* **1995**, *99*, 17087.
(31) Polihronov, J. G.; Hedstrom, M.; Hummel, R. E.; Cheng, H.-P. *J. Lumin.* **2002**, *96*, 119.
(32) Gritzner, G.; Selbin, J. *J. Inorg. Nucl. Chem.* **1968**, *30*, 1799.
(33) The formation of CC complexes most probably involves the ligation of the donor actinyl O in to the equatorial plane of the acceptor ion with the corresponding loss of a solvent water molecule. See Sullivan, J. C. *J. Am. Chem. Soc*. **1962**, *84*, 4256; Sullivan, J. C. *Inorg. Chem*. **1964**, *3*, 315; Murmann, R. K.; Sullivan, J. C. *Inorg. Chem*. **1967**, *6*, 892.
(34) See for example the reviews: Koltunov, V. S. *The Kinetics of the actinide reactions;* Atomizdat: Moscow, 1974; Cleveland, J. M. In *Plutonium Handbook A Guide to the Technology;* Wick, O. J., Ed.; American Nuclear Society: La Grange Park, IL,1980; Vol. 1 & 2, p 403. More recent studies: Koltunov and co-workers *Radiochim. Acta* **2004**, *92*, 387; *J. Nucl. Sci. Technol. Suppl.* **2002** *3*, 351; *Radiochim. Acta* **2002**, *90*, 1; *Radiochim. Acta* **1999**, *86*, 41.